Nuclear Physics A551 (1993) 378–408
North-Holland

NUCLEAR PHYSICS A

Shape transition of ^{146}Nd deduced from an inelastic electron-scattering experiment

R.K.J. Sandor[a], H.P. Blok[a,b], M. Girod[c], M.N. Harakeh[a], C.W. de Jager[b], V. Yu. Ponomarev[d] and H. de Vries[b]

[a] *Faculteit Natuurkunde en Sterrenkunde, Vrije Universiteit, De Boelelaan 1081, 1081 HV Amsterdam, The Netherlands*

[b] *Nationaal Instituut voor Kernfysica en Hoge-Energie Fysica, sectie K, P.O. Box 41882, 1009 DB Amsterdam, The Netherlands*

[c] *Service de Physique et Techniques Nucléaires, CEA, Bruyères-le-Châtel, BP 12, F-91680 Bruyères-le-Châtel, France.*

[d] *Laboratory of Theoretical Physics, Joint Institute for Nuclear Research Dubna, Head post office P.O. Box 79, Moscow, Russian Federation*

Received 15 July 1992

Abstract: Excited states in ^{146}Nd up to an excitation energy of 3.0 MeV were investigated by inelastic electron scattering in a momentum-transfer range of 0.5–2.8 fm^{-1}. Transition charge densities were extracted for natural-parity states with spins ranging from 0^+ up to 5^-. The experimental transition charge densities have been compared to microscopic calculations performed in the framework of the quasiparticle-phonon model (QPM) and the density-dependent Hartree-Fock-Bogoliubov model (DDHFB). The QPM assumes a spherical nucleus, whereas the DDHFB model is most suitable for strongly deformed nuclei. Both models are thus complementary in describing this transitional nucleus. On the basis of the DDHFB calculations it is shown that ^{146}Nd is softly deformed in its ground state; the agreement with the experimental data for the first excited 2^+ and 4^+ states indicates that at low excitation energies ^{146}Nd can be considered to be a deformed nucleus. This feature is also analysed and confirmed for the first excited 3^- and 5^- states by means of the macroscopic rotation-vibration model. At higher excitation energies the level structure is well predicted by the QPM. Moreover, all higher states observed in the experiment have transition charge densities peaking at the same radius. This is typical for spherical nuclei. Therefore, it is concluded that ^{146}Nd is slightly deformed at low excitation energies, but undergoes a shape transition at higher energies, turning spherical.

E NUCLEAR REACTIONS ^{146}Nd(e, e'), $E = 112$–450 MeV, $q = 0.5$–2.8 fm^{-1}; measured longitudinal form factor of low-lying states, Fourier-Bessel analysis, determined transition charge densities, compared to microscopic quasiparticle-phonon model and Hartree-Fock-Bogoliubov model calculations and macroscopic rotation-vibration model, deduced λ, J^π and $B(E\lambda)$ values.

1. Introduction

The nucleus ^{146}Nd lies in the middle of a chain of isotopes that is known to exhibit a shape transition from spherical at one end (^{142}Nd) to well-deformed at

the other (^{150}Nd). It is regarded as a transitional nucleus, since its exhibits both the features of vibrational nuclei, like a two-phonon triplet at approximately twice the excitation energy of the first 2^+ state, as well as the features of rotational nuclei, like an intrinsic quadrupole moment [1]) and an enhanced B(E2) value of the first 2^+ state. Consequently, realistic microscopic calculations are extremely complicated, because single-particle as well as collective degrees of freedom, which must include both vibrational and rotational motions, have to be accounted for. Indeed, until now there has been only one significant attempt, by von Bernus *et al.* [2]), to describe the level structure of ^{146}Nd microscopically. It has since then been recognized, that in order to be able to judge any model on its merits, more complete and accurate experimental details are necessary. This has led to a wealth of experiments performed in the last few years with many different probes, e.g. with the (n, n'γ) reaction [3]), $\gamma\gamma$-correlation measurements after thermal-neutron capture [4]) and (p, p') and (d, d') experiments [5]). From a Coulomb-excitation experiment [6]) and a photon-scattering experiment at low energy [7]) B(Eλ) values of some low-lying collective states were obtained.

Because of the well-understood relationship between the measured cross section in electron scattering and the radial transition densities, electron scattering is a well-suited tool to investigate the spatial properties of the nuclear wave function. Nuclear charge and current densities provide information about the dynamic properties of the various excitation modes and hence will reflect differences between various collective excitations.

In this paper the results of an inelastic electron-scattering experiment on ^{146}Nd are presented. The data were taken simultaneously with those published in previous papers on ^{142}Nd [refs. [8,9])] and ^{150}Nd [refs. [10,11])]. Some forty levels up to 3.0 MeV excitation energy have been observed and with the aid of the previously mentioned experiments the spin and/or parity of most excitations were identified. For thirteen of these levels transition charge densities were extracted, whereas for nine more levels B(Eλ) values have been determined.

An attempt has been made to interpret the results in terms of vibrations or rotations by comparing them to microscopic calculations. Two such models have been used: the quasiparticle-phonon model (QPM) and a density-dependent Hartree-Fock-Bogoliubov (DDHFB) model. In the QPM calculations a spherical mean-field potential has been assumed, so that deformation effects could not be accounted for. In contrast, the DDHFB model makes explicit use of a deformed potential and calculates variables such as moments of inertia, necessary for a fully dynamical calculation in the cranking approximation, which works best for strongly deformed nuclei. It is therefore expected that both models will have their deficiencies in describing the transitional nucleus ^{146}Nd. Nevertheless, until a hybrid microscopic model has been developed, which treats both vibrational and rotational degrees of freedom on an equal footing, the only way in which more insight can be gained into the structure of this class of nuclei is by comparing experimental data to the

results of calculations performed in these limiting cases and to investigate to what extent each model is appropriate. A third model, the macroscopic rotation-vibration model (RVM), was used to investigate if ^{146}Nd can indeed be regarded as a nucleus with both rotational and vibrational degrees of freedom.

The above-mentioned models have been extensively described in refs. [8-11]). Therefore, only the differences between those calculations and the present ones will be mentioned below. Similarly, the experimental procedures used in the analysis of the experimental data on ^{146}Nd are the same as those in the cited papers and the reader is referred to those. The only exception is that the transverse contribution to the cross section of the excited states was not measured specifically for ^{146}Nd. However, both in ^{142}Nd and in ^{150}Nd that contribution was deduced to be smaller than 2% for scattering angles smaller than 83°. Therefore, it is reasonable to assume that in the angular range of the present experiment the major contribution is from the charge form factor. Hence, the transverse component has been neglected in the analysis.

This paper is organized as follows: in sect. 2 the extensions and alterations made to the parameters of the two microscopic models are explained and discussed. In sect. 3 the experimental data for the quadrupole states are presented and compared to the results from the calculations. Sects. 4, 5 and 6 deal in the same manner with the octupole, the hexadecapole and the remaining states observed in the experiment, respectively. In sect. 7 the data are compared to the RVM calculations. Finally, in sect. 8 a summary and the conclusions are given.

2. Theoretical considerations

As mentioned in the Introduction, both the quasiparticle-phonon model (QPM) and the density-dependent Hartree-Fock-Bogoliubov method with dynamical calculation of transition charge densities (DDHFB) have been extensively described in previous papers on ^{142}Nd [refs. [8,9])] and ^{150}Nd [refs. [10,11])]. Therefore, only the differences with those presentations are discussed here, especially with respect to the parameters that are used.

For the QPM calculations the same radial parameters for the Woods-Saxon (WS) potential, taken from the (e, e'p) experiment of Lanen [12]), were used as for ^{142}Nd [ref. [9])], with a correction for the increase of the nuclear radius due to the extra neutrons. The derivative of the WS well is assumed for the radial dependence of the residual interaction. In principle, for each multipolarity the parameters $\kappa_{0,1}^{J^\pi}$ of the effective residual force are chosen to reproduce the experimental excitation energy and collectivity of the lowest state. To restrict the number of free parameters involved in the calculations the ratio $\kappa_1^{J^\pi}/\kappa_0^{J^\pi}$ was fixed at -1.2 for all J^π, based on previous experience with QPM calculations using Bohr-Mottelson residual forces in reproducing properties of low-lying states and giant resonances. However, for the excitations with a multipolarity of 5 and higher this leads to unrealistic values

of the isoscalar force $\kappa_0^{J^\pi}$. Therefore, for these excitations a different procedure was followed. For negative-parity states $\kappa_0^{J^\pi}$ was taken equal to the value of that of the octupole states, i.e. $\kappa_0^{3^-}$, and for positive-parity states the same value as for the quadrupole states, $\kappa_0^{2^+}$, was used.

A difficulty, encountered in the calculations for ^{146}Nd, is the strong coupling between the different one-, two- and three-phonon configurations. This strong coupling makes it necessary to include as many configurations as possible. However, limitations on computing time made it impractical to use a significantly larger basis than in the case of ^{142}Nd. In truncating the phonon basis we attempted to include all important configurations which might contribute to the structure of low-lying states below 3 MeV. Thus, all one-phonon configurations with $E_x \leqslant 4.0$ MeV, which represent the main contribution of the multipole strength in this region and also determine to a large degree the shape of the transition densities, and two-phonon configurations with $E_x \leqslant 5.5$ MeV, which cause the distribution of one-phonon strength over low-lying states, have been taken into account in the present calculations. Three-phonon configurations, constructed from the first collective 2^+, 3^-, 4^+ and 5^- one-phonon terms, were also included. It is clear that such a basis truncation limits the validity of the calculations for a nucleus with a strong coupling between configurations, especially for states at higher excitation energies. This results in the missing of some weak states for which the observation of the γ-decay cascade indicates important contributions of many-phonon configurations. However, in (e, e') scattering mainly states with a large contribution of one-phonon configurations are excited, which should correspond well with the results of this approximate framework.

The DDHFB calculations have been performed along the same lines as described in ref. [11]). A possible shortcoming of the model is the use of the cranking approximation in the calculation of the moments of inertia, which might not be applicable for the case of ^{146}Nd. Furthermore, the gaussian-overlap approximation was invoked in the calculation of the transition densities, although this approximation has only been proven correct for (strongly) deformed nuclei [13]). Nevertheless, in view of the rather good agreement for ^{150}Nd a reasonable reproduction of the data is expected for ^{146}Nd. Unfortunately, apart from the ground-state charge density, theoretical results are only available for two excited states, namely the 2_1^+ state and the 4_1^+ state.

Fig. 1 shows the potential-energy surface (PES) of ^{146}Nd. The static minimum is located at $\beta = 0.15$ and $\gamma = 7°$. This shows, that the nucleus already has a triaxial deformation in the ground state. A second minimum is located at $\beta = 0.10$ and $\gamma = 60°$, which corresponds to a pure oblate deformation. Both minima are quite soft, especially in the γ-direction, and the barrier between the two minima is not very high, indicating that the nucleus can easily change its shape when excited. The shallowness of the minima shows that a dynamical calculation is necessary for this nucleus.

The results of the DDHFB calculations are compared in fig. 2 with the elastic form-factor data and the resulting ground-state charge distribution, showing a

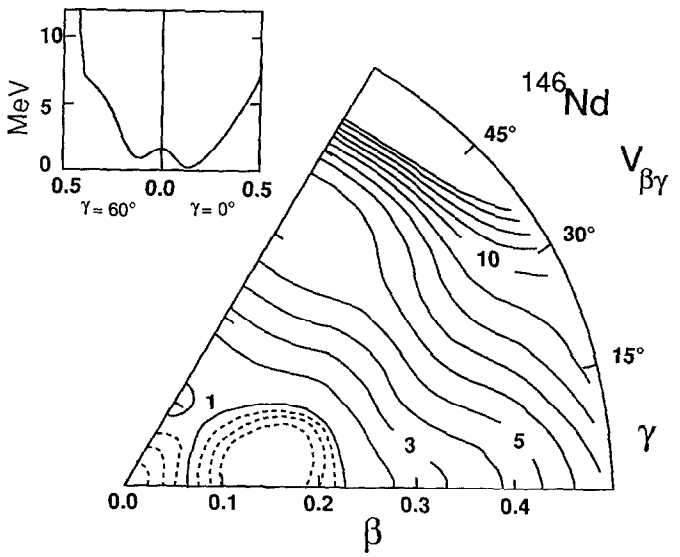

Fig. 1. Contour plot of the calculated potential-energy surface of ^{146}Nd. The inset represents cuts in the PES along $\gamma = 0°$ and $\gamma = 60°$.

satisfactory agreement. The discrepancy between the calculations and the experimental data is somewhat larger at the maximum of the experimental charge density than for ^{150}Nd. Although on the whole the description of the nuclear interior is better, the calculated density shows larger fluctuations than for ^{150}Nd. This suggests that, like in the case of ^{150}Nd, higher-order correlations between quasiparticles should be taken into account.

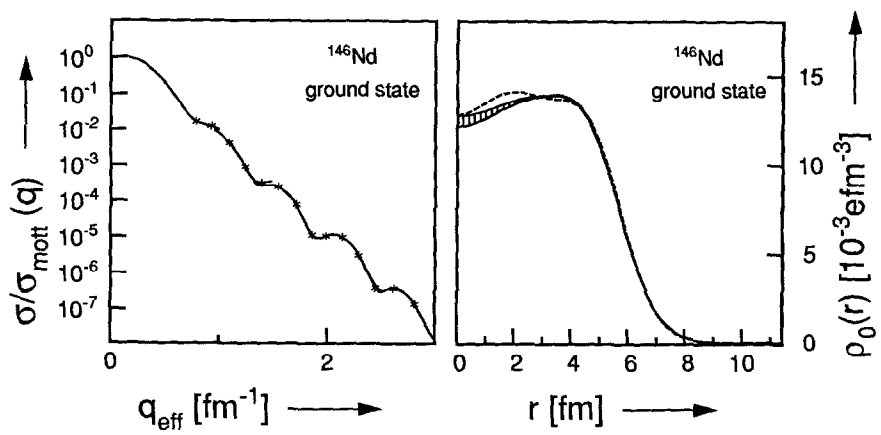

Fig. 2. The elastic form factor and the deduced experimental ground-state charge density of ^{146}Nd (curve with error band) compared with the results of the DDHFB calculations (dashed line).

3. The quadrupole states

In the present experiment eight states believed to be 2^+ states were observed. Table 1 lists the excitation energies and the $B(E2)$ values. The state at 1.303 MeV, identified in a β^- decay experiment [15]) as a 2^+ state, was observed only weakly at two q-values; therefore, no form factor is presented. The same is true for the quadrupole state at 1.789 MeV. For the levels at 2.198 and 2.976 MeV, the spin and parity assignments of which were taken from ref. [5]), only form factors are presented in fig. 3. In order to extract a $B(E2)$ value for the latter state a functional form was assumed for the transition charge density,

$$\rho^{(\lambda)}(r) \propto \frac{d\rho_0(r)}{dr} \tag{1}$$

with $\rho_0(r)$ given by a two-parameter Fermi distribution. The radial parameter was always adjusted for good agreement with the form-factor data. The skin-thickness parameter was taken from ref. [16]). Such a transition density is usually known as a one-phonon density. Following the nomenclature of ref. [9]), the name standard density is used henceforward.

The adjusted radial parameter of the standard density for the state at 2.976 MeV resulted in a transition charge density that peaks at a radius of 6.2 fm. By adjusting its strength such that the first maximum of the experimental form factor was well

TABLE 1

Excitation energies and $B(E2)$ values of the 2^+ states observed in the present experiment compared to those from the literature and the QPM calculations. Above 2 MeV only excitation energies are given of those levels which have also been observed in the present experiment. Energies of states which could not be measured accurately enough are given without errors.

Literature [a])		Present experiment		QPM calculations		
E_x [MeV]	$B(E2)$ [e^2fm^4]	E_x [MeV]	$B(E2)$ [e^2fm^4]	ν	E_x [MeV]	$B(E2)$ [e^2fm^4]
0.45386	$6.91\,(5)\times10^3$ [c])	0.453 (6)	$6.91\,(5)\times10^3$ [d])	1	0.565	5.44×10^3
1.3032		1.303		2	1.640	2.42×10^1
1.4706		1.470 (5)	$6.8\,(5)\times10^2$	3	2.150	1.06×10^3
1.7874		1.789		4	2.360	1.84×10^1
1.9054				5	2.490	2.66×10^{-2}
1.9779		1.977 (9)	2×10^2 [e])	6	2.600	2.08×10^2
2.199 [b])		2.198		7	2.980	1.82×10^2
2.665 [b])		2.665 (10)	$1.68\,(20)\times10^2$	8	3.380	9.77×10^1
2.974 [b])		2.976	6×10^1 [f])	9	3.430	2.80×10^2

[a]) Ref. [14]).
[b]) Spin and parity assignments taken from ref. [5]).
[c]) Taken from ref. [6]).
[d]) $B(E2)$ value from ref. [6]) used as a data point.
[e]) $B(E2)$ value obtained assuming a standard transition density shifted to 5.0 fm.
[f]) $B(E2)$ value obtained assuming a standard transition density.

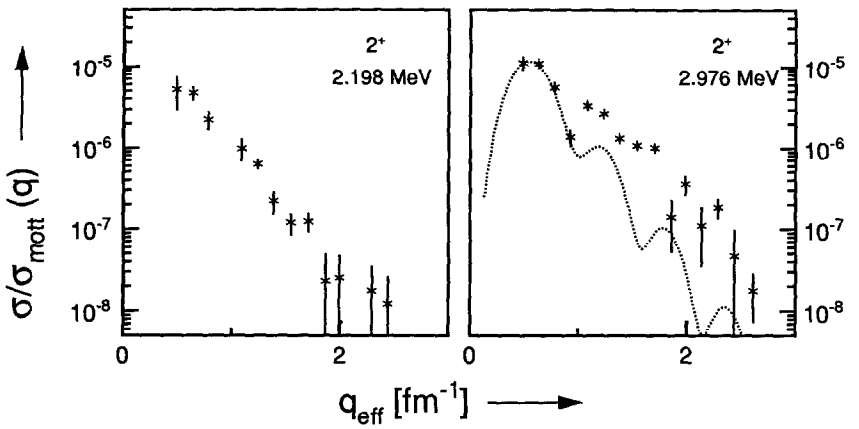

Fig. 3. Form factors of the 2^+ states with excitation energies of 2.198 and 2.976 MeV. The dotted curve represents a fit with a standard density.

described, a B(E2) value of 60 e^2fm^4 was obtained. The state at 1.977 MeV could only be resolved from the 4^+ state at 1.987 MeV for the lowest four q-values. A good fit to these data could be obtained with a standard density that peaked at 5.0 fm. Such a small value for the radial parameter is supported by the QPM calculations, as will be discussed below. For the other three quadrupole states transition charge densities were extracted, which are depicted in fig. 4 together with the experimental form factors. The first form-factor minimum of the 2^+ state at 2.665 MeV is clearly filled, which points to contributions from other states.

As mentioned in sect. 2, the relatively simple picture which existed for ^{142}Nd in terms of phonon excitations is no longer valid in ^{146}Nd. Due to the strong coupling between one- and multi-phonon states and hence the redistribution of the strength of the quasiparticle RPA one-phonon configurations over many states, all excitations to be discussed below have very complicated structures. This is illustrated in table 2, where the configurations contributing to the 2_1^+ states of ^{142}Nd and ^{146}Nd, respectively, are listed. The structure in terms of phonon configurations of states at higher energies is even more complicated. Therefore, only the main features of the excitations will be discussed in the comparison of the QPM with the experimental results, while the connection to the RPA results will be omitted.

Table 1 lists the excitation energies and B(E2) values of the quadrupole states as calculated by the QPM and fig. 5 shows the transition charge densities calculated for the first six 2^+ states. The strength distribution of these states as predicted by the QPM is more or less confirmed by the experimental results. There are three rather strong 2^+ states, i.e. the 2_1^+, 2_3^+ and 2_6^+ states, and three weak ones which are hardly seen in the present experiment. A comparison of the experimental and the calculated transition charge densities for the 2_1^+ state, depicted in fig. 4, immediately indicates that the nucleus ^{146}Nd displays deformation effects. Although the radial

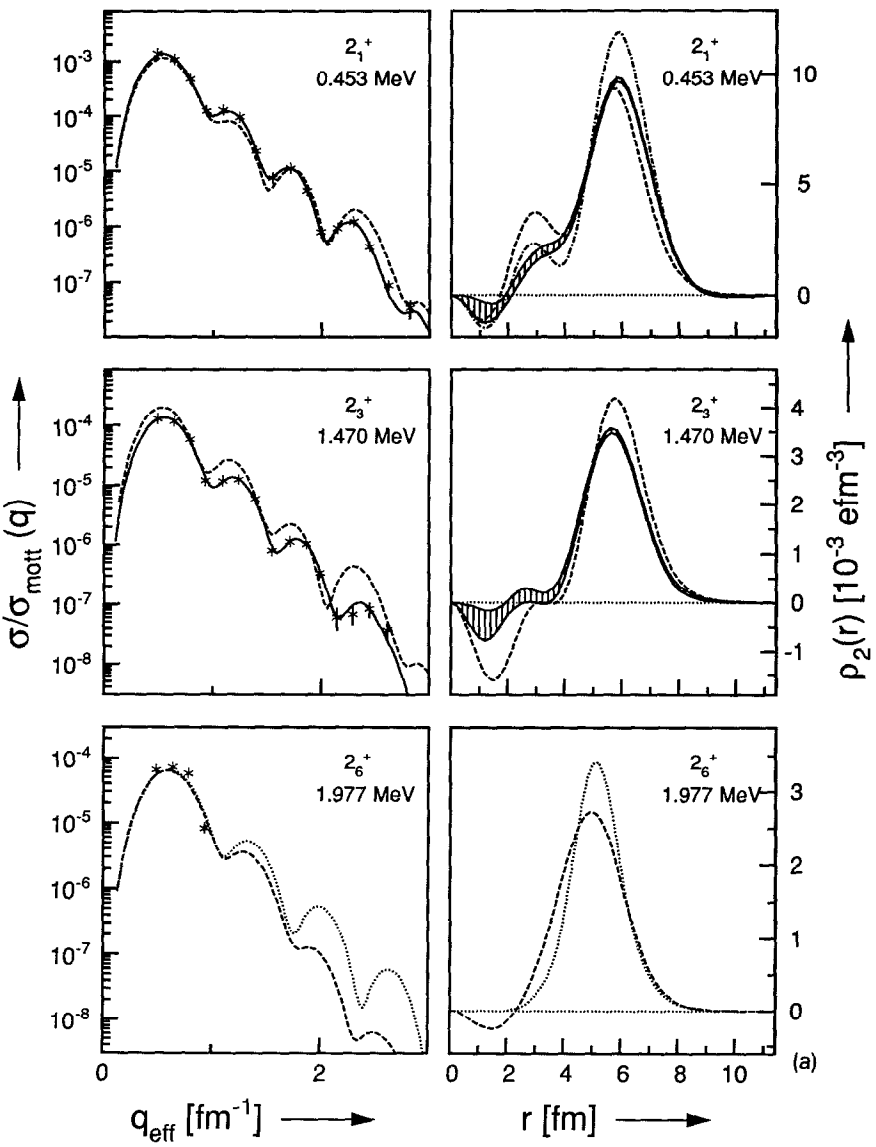

Fig. 4. Experimental transition charge densities (curves with error bands) and form factors of the 2^+ states at 0.453, 1.470, 1.977 and 2.665 MeV. The solid curves represent the Fourier-Bessel fits, whereas the dotted curve is the result of a fit with a standard transition density shifted to 5.0 fm. The calculations by the QPM are represented by the dashed curves and the DDHFB results by the dot-dashed curve.

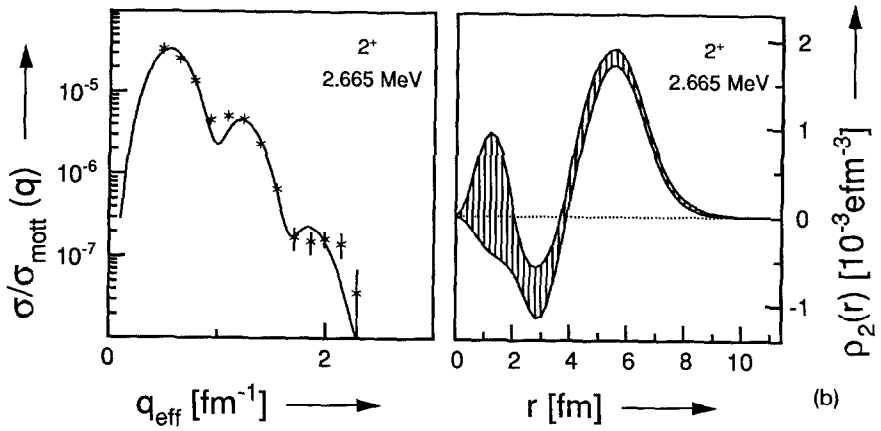

Fig. 4—continued

parametrisation of the Woods-Saxon potential for ^{142}Nd taken from ref. [12]) has been corrected for the assumed increase in size because of the four extra neutrons, an extra increase of 0.15 fm is observed in the radius at which the experimental transition charge density peaks in comparison to the one obtained with the QPM. The general features of the density are reasonably well reproduced, with a relatively weak structure in the nuclear interior. In fig. 4 the results of the dynamical DDHFB calculations are also displayed. They agree very well with the experimental results as far as the shape is concerned, although the strength of the transition is overestimated, even more than in the case of ^{150}Nd.

The description of the 2_3^+ state by the QPM, also shown in fig. 4, is quite good. The main contribution to this state is from the $[2_1^+ \times 4_1^+]^{(2)}$ two-phonon configuration, which has shifted to a low energy due to the interaction with three-phonon configurations. The two-phonon contribution in the nuclear interior is practically cancelled by destructive interference with other configurations. The remaining contributions come (among others) from the collective first and second one-phonon states. This

TABLE 2

The contributions of the different types of phonon configurations to the first 2^+ state in ^{142}Nd and ^{146}Nd. The percentages are the sums of contributions larger than 1%.

	^{142}Nd		^{146}Nd	
Type	# configurations	%	# configuartions	%
one-phonon	1	91.6	2	72.8
two-honon	2	4.8	4	21.7
three-phonon			2	3.6

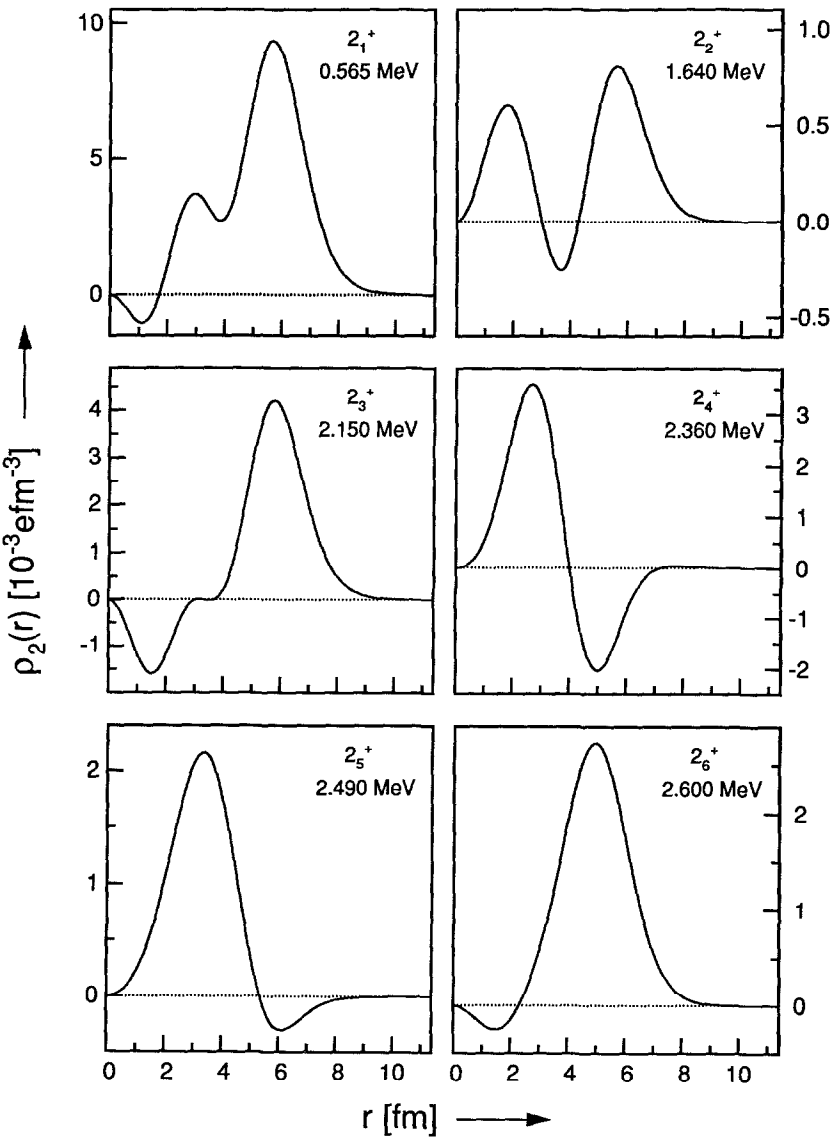

Fig. 5. Transition charge densities of the first six 2^+ states calculated with the QPM.

altogether results in a surface-peaked transition charge density. Therefore, it may be concluded that the 2_3^+ state is still quite collective, in spite of the fact that the experimental B(E2) value is an order of magnitude smaller than that of the 2_1^+ state.

An interesting feature is that the radius, at which the transition charge density of the 2_3^+ state has its maximum, is somewhat smaller than predicted by the QPM. This can be the result of nuclear deformation. Indeed, this transition can be well described in the macroscopic RVM as an excitation of the 2^+ member of the γ-band, as will be shown in sect. 7.

As mentioned earlier, the 2_6^+ state was experimentally resolved from the neighbouring 4^+ state only at the four lowest q-values, i.e. up to 0.95 fm^{-1}. However, the form factor calculated from the QPM transition charge density describes the data well. This seems to indicate that the collectivity and the structure of this state, consisting mainly of the fourth one-phonon configuration and only little multi-phonon contributions, is reasonably predicted.

All in all, the description of the quadrupole states up to 2.0 MeV is reproduced rather well by the QPM. Although a small onset of deformation can be deduced from the radial positions at which the transition charge densities of the 2_1^+ and 2_3^+ states peak, the other quadrupole states, and in particular the 2_6^+ state, seem to be governed by the vibrational (phonon) degrees of freedom. The discrepancy between the excitation energies predicted by the QPM and those observed in the experiment is similar to the case of ^{142}Nd.

The calculated quadrupole states at higher excitation energies could not be assigned to experimental transitions, due to the high level density above 2 MeV. For the transition charge density of the quadrupole state at 2.665 MeV no comparison with a calculated density is possible, since the state is believed to be outside the range of validity of the present QPM calculations.

4. The octupole states

Transition charge densities were extracted for two 3^- states, at 1.190 and at 2.339 MeV. These are depicted in fig. 6, together with the respective form factors. The B(E3) value of $3.52(21)\times10^5 e^2\text{fm}^6$ of the 3_1^- state obtained in the present experiment is considerably larger than the value of $2.6(3)\times10^5 e^2\text{fm}^6$ quoted in ref. [17]). For three more states, those at 2.530, 2.690 and 2.850 MeV, a Fourier-Bessel analysis was not possible, since the form-factor data show a clear filling of the diffraction minima, as depicted in fig. 7. If this is due to admixtures from excitations that are much weaker or of a higher multipolarity, the first form-factor maxima of the octupole states will not be affected. Under this assumption a B(E3) value was determined by taking the shape of a standard density for the transition charge density and adjusting its stength. The deduced excitation energies and B(E3) values are listed in table 3. Several other possible 3^- states between 2.8 and 3.0 MeV have been observed, but only at a few q-values. Hence, these form factors are not presented

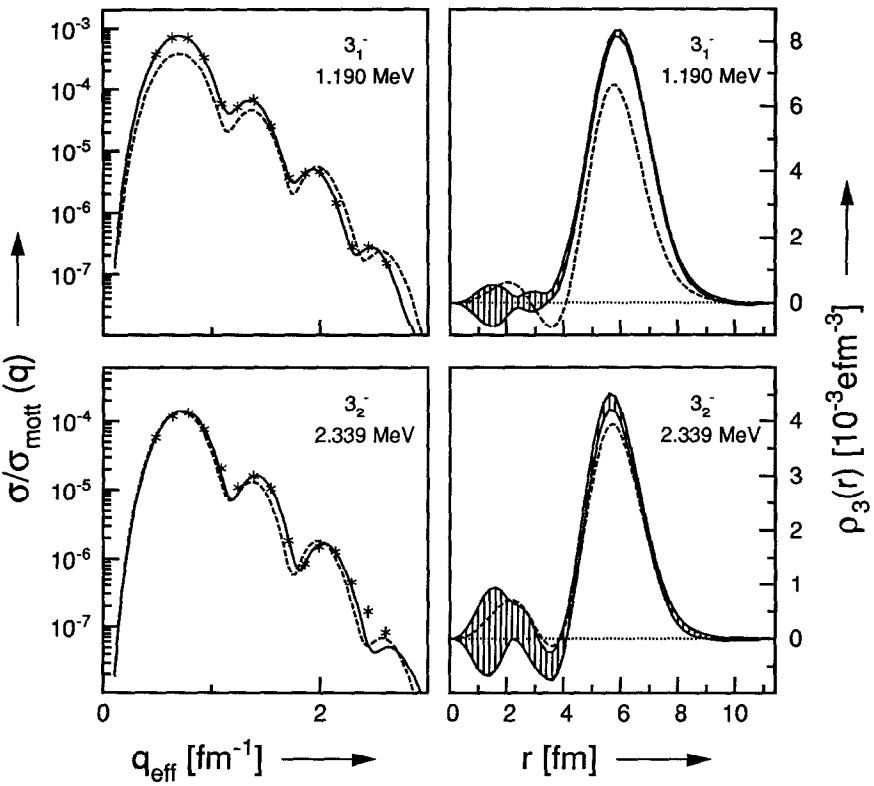

Fig. 6. Experimental transition charge densities (curves with error bands) of the 3_1^- state at 1.190 MeV and the 3^- state at 2.339 MeV and the respective form factors with the Fourier–Bessel fits (solid lines). The dashed curves represent the QPM calculations.

here. The multipolarities have been taken from Pignanelli *et al.* [5]), in which all states listed in table 3 were identified as octupole states.

The QPM predicts only six octupole states up to an excitation energy of 4 MeV, much fewer than observed experimentally. This underestimation of the number of 3^- states by the QPM also occurs in the case of ^{144}Nd [ref. [18])]. One possible explanation for this discrepancy is that in nuclei away from closed shells QPM calculations should be performed up to an excitation energy higher than 4.0 MeV. Another explanation could be that only a limited number of multi-phonon states were included in the calculations. In general, the inclusion of higher-order correlations would push the roots of the RPA equation down in energy. This would increase the number of octupole states in the region of excitation investigated in this experiment. However, this would not change the structure of the low-lying octupole states very much, which means that the structure and the strength of the densities such as presented for the first two 3^- states are largely independent of the truncation of the two- and three-phonon basis.

TABLE 3

Excitation energies and B(E3) values of the 3^- states observed in the present experiment compared to values from the literature. Energies of states which could not be measured accurately enough are given without errors.

Literature	Present experiment		QPM calculations		
E_x [MeV]	E_x [MeV]	B(E3) [e^2fm^6]	ν	E_x [MeV]	B(E3) [e^2fm^6]
1.1895 [a])	1.190 (6)	$3.52\,(21)\times10^5$	1	1.150	1.62×10^5
2.1673 [a])					
2.336 [b])	2.339 (8)	$5.1\,(7)\times10^4$	2	2.380	5.34×10^4
2.527 [b])	2.530 (8)	2×10^4 [c])	3	3.010	4.92×10^2
2.685 [b])	2.690	5×10^3 [c])	4	3.180	6.26×10^3
2.805 [b])	2.807		5	3.390	3.71×10^4
2.820 [b])	2.822		6	3.840	1.05×10^4
2.846 [b])	2.850 (12)	2×10^4 [d])			

[a]) From ref. [14]).
[b]) From ref. [5]).
[c]) B(E3) value obtained using a standard density.
[d]) B(E3) value obtained using a standard density shifted to 6.0 fm.

The calculated transition charge densities for the states at 1.190 and at 2.339 MeV are shown in fig. 6 and their B(E3) values are listed in table 3. It is interesting to note that the densities of these octupole states show a similar structure, the main contribution for both states coming from the first one-phonon configuration and the $[2_1^+\times3_1^-]$ two-phonon configuration. This is in reasonable agreement with the results of the present experiment, as can be observed in fig. 6. It must be mentioned though, that the literature reports another 3^- state at 2.167 MeV [ref. [4])], which would make the level at 2.339 MeV the third 3^- state. However, the level at 2.167 MeV has not been observed, either in the present experiment or in the experiments of Pignanelli *et al.* [5]). Moreover, in an accurate (n, n′γ) experiment by Al-Janabi *et al.* [3]) this state is given a tentative 2^+ assignment. This means, that the experimental situation is not yet resolved, but that if the level at 2.167 MeV is indeed an octupole state, it cannot be the collective one predicted by the QPM. Furthermore, a close inspection of the experimental transition charge densities reveals that the transition density of the 2.339 MeV level peaks at a a smaller radius than that of the 1.190 MeV level, just as in the case of the quadrupole states. Since both levels are quite collective, it would be reasonable to assume that both densities peak at the nuclear surface. This indicates a possible deformation of the nucleus ^{146}Nd, such that the 3_2^- state at 2.339 MeV is a member of yet another octupole band, which in its turn implies that this state might be outside the model space of the present version of the QPM, despite the good agreement with the experimental transition charge density.

For the higher 3^- states the connection between the experiment and the calculations is not very clear. On the basis of their strengths, the states at 2.530 and 2.690 MeV may correspond to the calculated 3_5^- and 3_6^- states, respectively, which

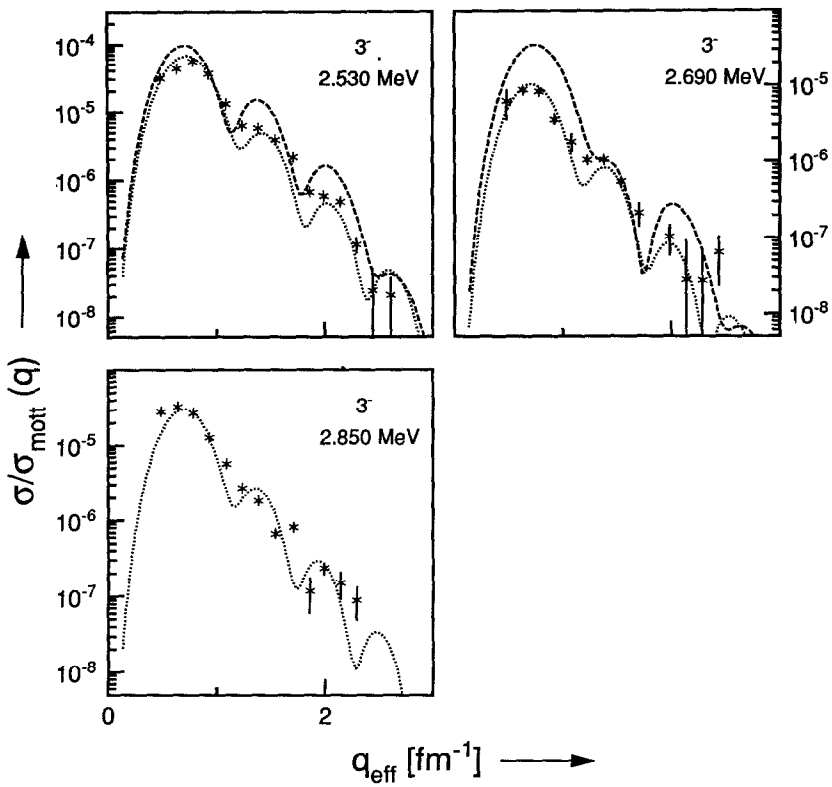

Fig. 7. Experimental form factors of the 3^- states at 2.530, 2.690 and 2.850 MeV. The dotted curves show fits obtained with standard transition densities. The results of the QPM calculations (dashed curves) are also shown.

would lead to the correct strength systematics. Since no experimental transition charge densities are available, comparison is only possible on the form-factor level. The positions of the calculated form-factor maxima, as shown in fig. 7, are in reasonable agreement with the experimental data.

5. The hexadecapole states

Of the excited states of ^{146}Nd observed in the present experiment, five were identified with the aid of the literature as 4^+ states. Two additional possible 4^+ states were observed in the spectra at only a few q-values. The excitation energies and $B(E4)$ values are listed in table 4. The 4^+ state at 1.987 MeV and the - in strength comparable - 2_6^+ state at 1.977 MeV could only be resolved at the lowest four q-values. As mentioned in sect. 3, the QPM results suggest a transition charge density for the 2_6^+ state which seems to be consistent with the measured form factor up to 1.0 fm^{-1} and has the shape of a standard density shifted to 5.0 fm. The 2_6^+ contribu-

TABLE 4

Excitation energies and B(E4) values of the 4^+ states observed in the present experiment compared to values from the literature. Energies of states which could not be measured accurately enough are given without errors.

Literature [a]	Present experiment		QPM calculations		
E_x [MeV]	E_x [MeV]	B(E4) [e^2fm^8]	ν	E_x [MeV]	B(E4) [e^2fm^8]
1.04317	1.044 (10)	$1.50\,(26)\times10^6$	1	0.870	1.42×10^6
1.7451	1.747 (9)	$3.61\,(32)\times10^6$	2	1.590	2.33×10^6
1.9189	1.919				
1.9893	1.987 (9)	$2.1\,(4)\times10^6$	3	2.040	2.19×10^6
2.550 [b]			4	2.340	1.64×10^5
2.620 [b]	2.622 (12)	3×10^5 [c]	5	2.450	1.98×10^5
2.930 [b]	2.935 (10)	$1.6\,(6)\times10^6$	6	2.520	1.83×10^5
			7	2.580	1.15×10^5
			8	3.010	1.29×10^6
			9	3.330	1.55×10^4

[a]) From ref. [14]).
[b]) From Pignanelli *et al.* [5]).
[c]) Obtained using a standard transition density.

tion, calculated with this standard transition density, was then subtracted from the form factor of the doublet. The resulting form factor of the 4_4^+ state and the extracted transition charge density are shown in fig. 8, together with the form factors and transition charge densities of the other hexadecapole states. The data of the state at 2.622 MeV were analysed with a standard transition density because of the filling of the diffraction minima.

The hexadecapole states in ^{146}Nd display several interesting features. First, the transition charge density of the 4_1^+ state peaks at a large radius than that of the 2_1^+ state, just as in ^{150}Nd. Again, this points to a positive hexadecapole moment of the nucleus. This is in agreement with the calculations of Götz *et al.* [19]), who predict $\beta_4 = 0.056$. Second, the transition charge density of the 4_2^+ state has a similar shape as that of the 4_1^+ state (see fig. 8), but with an inward shift of 0.7 fm. This might be due to an excitation of the γ-band. However, if the notion of bands is introduced in ^{146}Nd, then one would expect the 2_3^+ state at 1.470 MeV, the only candidate for the 2^+ state of the γ-band, to be shifted inward by the same amount. Although a shift of approximately 0.2 fm is visible, it is much smaller than the 0.7 fm observed for the hexadecapole states. It might be argued, that in the process of exciting the 4_2^+ state the hexadecapole deformation of the nucleus disappears due to a rearrangement of the nucleons inside the nucleus. This would imply that the nucleus is very soft with respect to hexadecapole excitations. Calculations in the framework of the DDHFB model should be able to answer these questions. Indeed, for the ground-state band DDHFB calculations predict densities for the 2_1^+ and the 4_1^+ states, shown in figs. 4 and 8, respectively, that are in reasonably good agreement with the

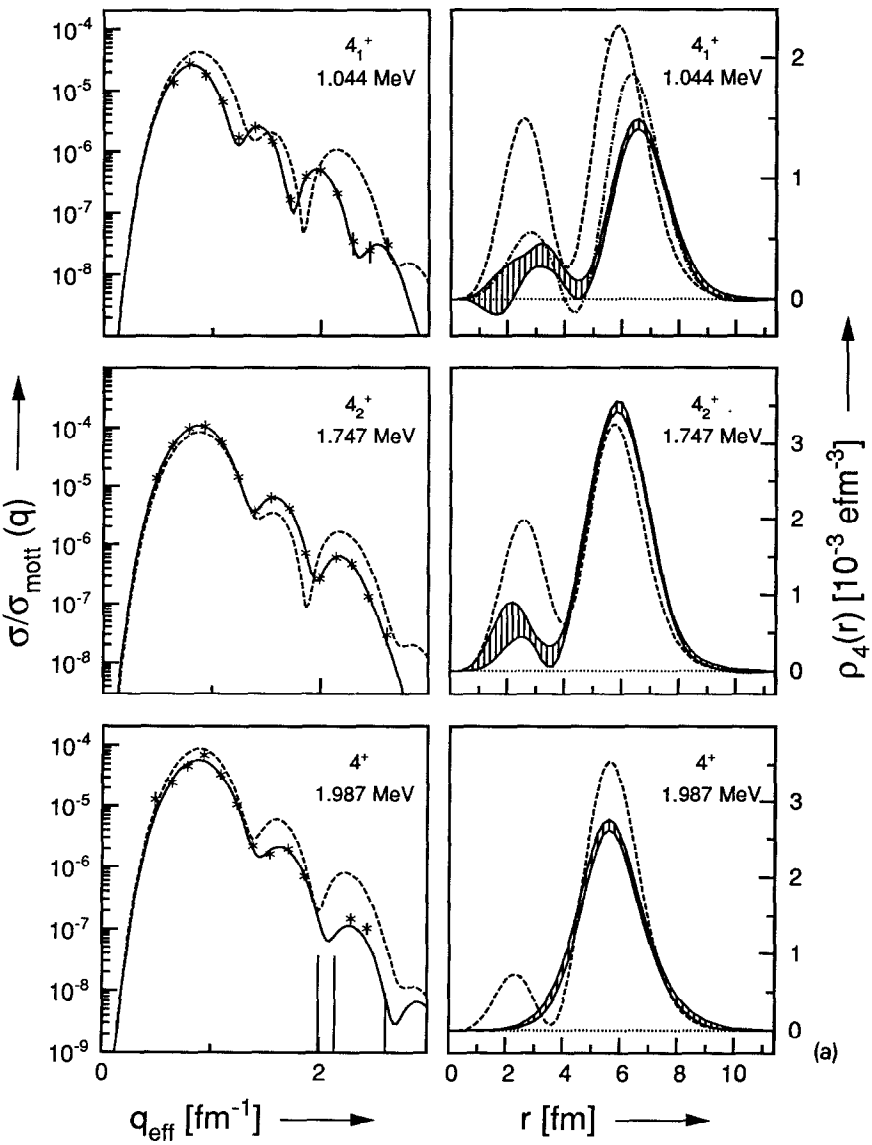

Fig. 8. Comparison between the experimental and the theoretical results for the hexadecapole states in ^{146}Nd. Shown are the experimental transition charge densities (curves with error bands) of the 4_1^+ state at 1.044 MeV, the 4_2^+ state at 1.747 MeV, the 4_4^+ state at 1.987 MeV (after subtraction; see text) and the 4^+ state at 2.935 MeV and their respective form factors. The solid curves show the Fourier-Bessel fits. The calculations by the QPM are represented by the dashed curves and the DDHFB results by the dot-dashed curve. The form factor of the 4^+ state at 2.622 MeV is also shown, together with the fit (dotted curve) obtained with the standard transition density.

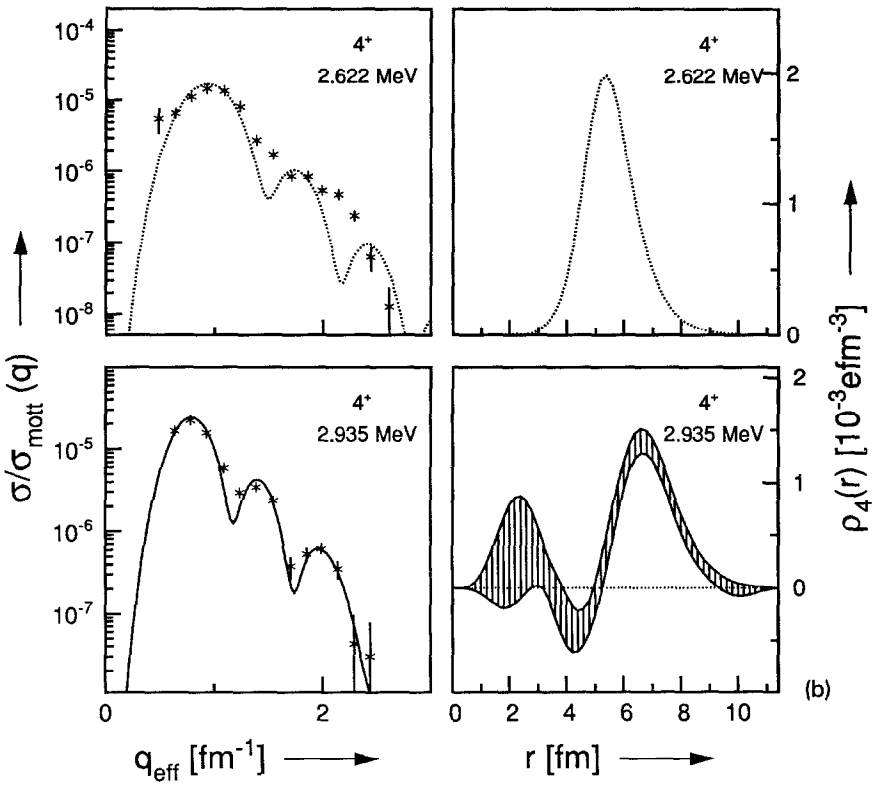

Fig. 8—continued

characteristics of the experimental data. Both the general structure and the shift of the transition charge density of the 4_1^+ state with respect to that of the 2_1^+ state are reproduced, although the shift is somewhat underestimated and a larger collectivity is predicted. Unfortunately, the DDHFB results for the γ-band are not yet available.

A third interesting feature of the hexadecapole states is the strength of the 4_2^+ state, which is nearly three times larger than that of the 4_1^+ state. Ichihara *et al.* [20]) have shown for other (well) deformed nuclei in the rare-earth region, that this might be due to a large effect of the Y_{42} term in the multipole operator which couples the 4_γ^+ state directly to the ground state. To investigate this point further, macroscopic calculations have been performed with the rotation-vibration model (RVM). Those results will be discussed in sect. 7.

Table 4 lists the B(E4) values and the excitation energies as calculated by the QPM. Here too, the large strength of the 4_2^+ state with respect to the 4_1^+ state is reasonably reproduced. The explanation of this feature is found in the underlying configurations of both states. Due to the interaction with the three-phonon terms, the $[2_1^+ \times 2_1^+]^{(4)}$ two-phonon pole of the RPA calculations is strongly shifted in energy from 3.75 to 1.04 MeV, a value lower than that of the first one-phonon pole at

2.030 MeV. This leads to the 4_1^+ state having a two-phonon contribution of 50% and a three-phonon contribution of 30%, in spite of the low energy of this state. In contrast, the 4_2^+ state has a 20% contribution of the first 4^+ one-phonon component, 45% of the $[2_1^+ \times 4_1^+]^{(4)}$ two-phonon configuration (also shifted from 3.46 to 1.81 MeV) and 20% of the three-phonon configuration. The major part of the strength of the first 4^+ one-phonon state is located in the calculated 4_3^+ state. This implies that the isoscalar strength parameter of the residual interaction must be adjusted for the 4_3^+ state to coincide with its experimental counterpart. The only excited state which is a suitable candidate on the basis of the large B(E4) value, is the state at 1.987 MeV. If one assumes that the calculated 4_3^+ state can be identified with the experimental state at 1.987 MeV, the excitation energies are observed to be practically identical, indicating that the $\kappa_0^{4^+}$ parameter has a realistic value. However, this excitation is experimentally known to be the 4_4^+ state, implying that a weakly excited state is missed by the calculations.

In fig. 8 the results of the QPM calculations are compared to the experimental data. Needless to say, the large radius at which the experimental transition charge density of the 4_1^+ state peaks is not reproduced by the calculations. However, its shape and strength are predicted reasonably well. The agreement for the 4_2^+ and the 4_4^+ states is also quite good, although it must be kept in mind that there is some ambiguity in the shape of the latter transition charge density due to the presence of the 2_6^+ state.

6. Other multipolarities

Some sixteen more peaks other than those discussed above have been observed in the spectra of ^{146}Nd. An attempt has been made to link the states observed in the present experiment to those seen in other experiments. However, due to the high level density above 2 MeV and the limited resolution it seems likely that many of the peaks observed correspond to doublet states. Only those states, for which the form-factor data show the features of a single excitation, will be discussed below. For other peaks only the excitation energies are listed in table 5 and the form factors, as far as the peaks were observed over a reasonable q-range, are shown in fig. 9 without any further discussion.

6.1. MONOPOLE STATES

Three 0^+ states up to 2.0 MeV are known in the literature. None of these has been observed in the present experiment. Especially interesting in this respect is that the 0_2^+ state, claimed to be observed [15]) at 0.916 MeV, has not been observed in any of the other experiments performed, although one would *a priori* expect for this nucleus a low-lying excited 0^+ state with vibrational features. At a higher energy, 2.231 MeV,

TABLE 5

Excitation energies and $B(E\lambda)$ values of states of multipolarities, different from $\lambda = 2$, 3 and 4, observed in the present experiment compared to values from the literature. Energies of states which could not be measured accurately enough are given without errors.

Literature [a]		Present experiment			QPM		
J^π	E_x [MeV]	J^π	E_x [MeV]	$B(E\lambda)$ [$e^2fm^{2\lambda}$]	J^π_ν	E_x [MeV]	$B(E\lambda)$ [$e^2fm^{2\lambda}$]
0^+	2.226 [b]	(0^+)	2.231	$3.84(81)\times10^{1}$ [c]			
1^-	1.3767	1^-	1.379 (6)	$4.51(27)\times10^{-3}$ [d]			
(1^-)	2.270 [b]		2.275				
5^-	1.5177	5^-	1.517 (6)	$2.64(29)\times10^{8}$	5^-_1	1.670	1.91×10^{8}
5^-	2.0458						
5^-	2.573 [b]	(5^-)	2.570	8.5×10^{7} [e]	5^-_2	2.520	5.25×10^{7}
5^-	2.747 [b]	5^-	2.748 (9)	$2.93(45)\times10^{7}$	5^-_3	3.120	4.52×10^{7}
		(5^-)	2.877 (19)		5^-_4	3.170	1.39×10^{7}
4^+	2.917 [b]	$(5^-, 6^+)$	2.915	4.7×10^{7} [e]	5^-_5	3.510	1.97×10^{7}
5^-	3.005 [b]	(5^-)	3.000	2.7×10^{7} [f]	5^-_6	3.810	1.83×10^{7}
7^-	2.0295		2.030				
$(4)^+$	2.0961		2.090 (9)				
$(1, 2^+)$	2.1489		2.152 (11)				
			2.374				
	2.4349		2.437				
2^+	2.4572		2.457				
	2.4835		2.484				
	2.7098		2.709				

[a]) From ref. [14]).
[b]) From ref. [5]).
[c]) In units of e^2fm^4.
[d]) $B(E1)$ value taken from ref. [7]) and used in the fit as a data point.
[e]) $B(E5)$ value obtained using a standard density peaking at 6.0 fm.
[f]) $B(E5)$ value obtained using a standard density peaking at 5.8 fm.

a state has been observed which was identified in (p, p′) and (d, d′) experiments [5]) as a possible monopole state. Its form factor and deduced transition charge density are shown in fig. 10. It should be remarked, that the Fourier-Bessel fit through the data is not very good.

6.2. DIPOLE STATES

Fig. 11 shows the transition charge density and the form factor of the 1^- state observed at 1.379 MeV. The $B(E1)$ value taken from ref. [7]) was used as a data point in the fit. The QPM predicts only one 1^- state in this energy region, of which the main contribution to the structure is from the two-phonon configuration $[2^+_1 \times 3^-_1]^{(1)}$

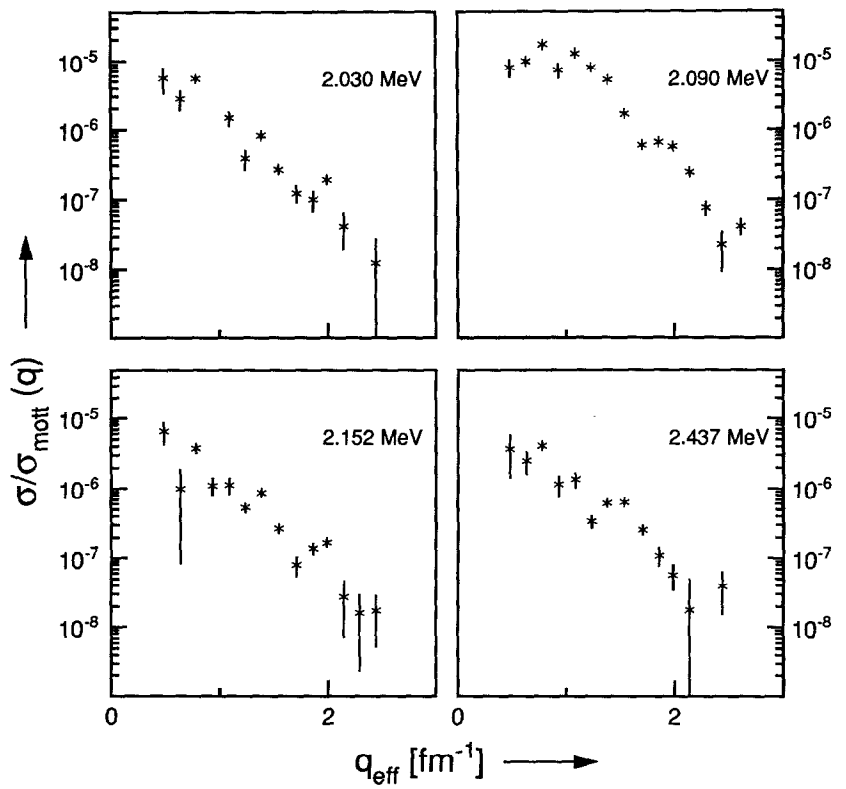

Fig. 9. Form factors of the states observed in the present experiment at 2.030, 2.090, 2.152 and 2.437 MeV which are not compared directly to QPM calculations.

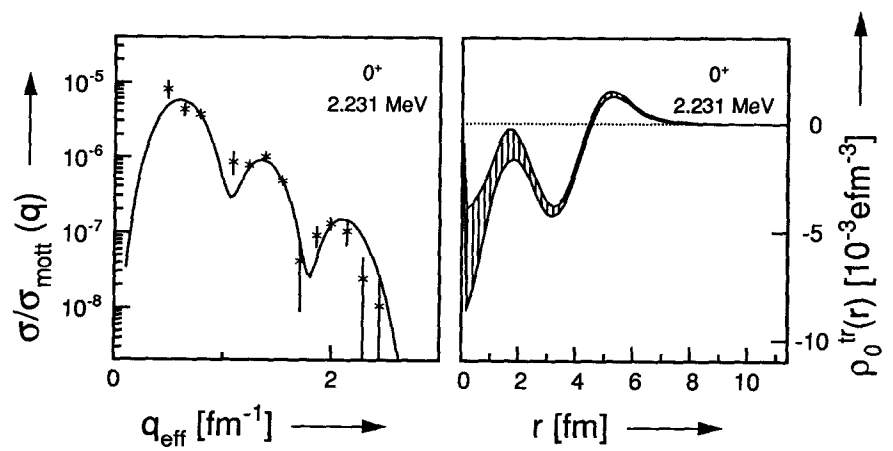

Fig. 10. Experimental form-factor data with the Fourier–Bessel fit (solid line) and the deduced transition charge density of the possible 0^+ state at 2.231 MeV.

since the first one-phonon 1^- configuration is located around 7 MeV. The transition charge density of the 1_1^- state is not well described by the QPM (see fig. 11). Although the shape is reproduced reasonably well, the strength is underestimated by about an order of magnitude. The QPM approach used here has a limited application in the description of states with little contribution from one-phonon configurations. For example, a more detailed treatment of ground-state correlations is necessary. Thus, the disagreement with the data is not surprising.

Another possible 1^- state at 2.275 MeV has been reported in ref. [5]). The form-factor data as observed in the present experiment are shown in fig. 11. Although this state is rather strongly excited for momentum transfers larger than 1.0 fm^{-1}, it is impossible to confirm the spin and parity assignment or perform a Fourier-Bessel analysis for this state due to the lack of low-q data. Nevertheless, the shape of the form factor is more consistent with that of a transition of higher multipolarity. This is supported

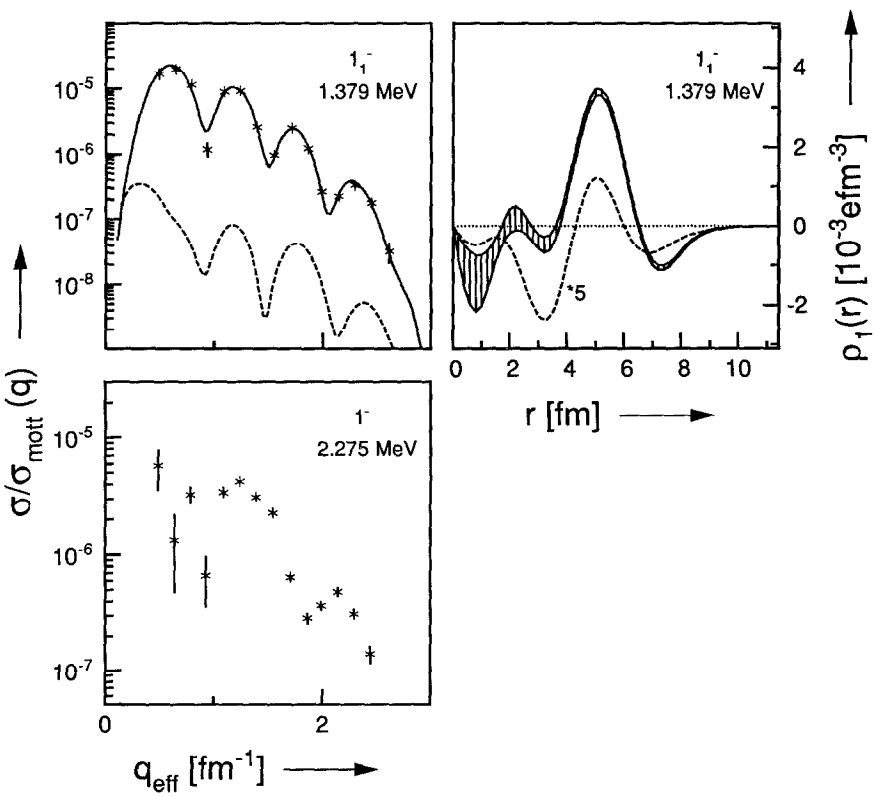

Fig. 11. Experimental form-factor data with the Fourier-Bessel fit (solid line) and the deduced transition charge density of the 1^- state at 1.379 MeV, together with the calculations by the QPM (dashed curves). For plotting purposes the transition charge density obtained from the QPM has been multiplied by 5. The form-factor data of the possible 1^- state at 2.275 MeV are also shown.

by the fact that the state has not been observed by Pitz *et al.* [7]), indicating that the B(E1) value must be very small.

6.3. HIGH-MULTIPOLARITY STATES

Four states known to be 5^- states have been identified as such. For two of them, the state at 1.517 MeV and the one at 2.748 MeV, transition charge densities have been extracted. They are shown, together with the corresponding form-factor data and the form factor of the 5^- state at 2.570 MeV, in fig. 12. Again, as in the case of the hexadecapole states, the transition charge density of the 5_1^- state peaks at a strikingly large radius, whereas that of the 5^- state at 2.748 MeV peaks at a value which would be expected if the nucleus would have a spherical shape. Also the form factor of the 5^- state at 2.570 MeV has a first maximum at the same value as the one at 2.748 MeV. The large width of the form-factor maximum of the state at 2.570 MeV does allow a larger radius for the peak of the transition density, but this feature can also be attributed to a contribution of another state. The B(E5) value listed in table 5 has been derived with a standard transition charge density peaking at the nuclear surface.

The 5^- state at 3.000 MeV has also been observed and its form factor is shown in fig. 13. Its B(E5) value listed in table 5 has been obtained with a fit using a standard transition density but with a smaller radius of 5.8 fm. Two more states have been observed that have form factors with a shape of a high multipolarity transition, i.e. the states at 2.877 and 2.915 MeV, also shown in fig. 13. The state at 2.915 MeV has been reported [5]) as a 4^+ state, but the form factor is more consistent with that of a 6^+ state or perhaps a 5^- state. The state at 2.877 MeV has not yet been identified in the literature. In this case an assignment of $J^\pi = 5^-$ seems most likely.

As in the case of the hexadecapole states, one is tempted to introduce a band structure in ^{146}Nd similar to that of ^{150}Nd, where the transition charge density of the 5_1^- state also peaks at a radius about 1 fm larger than that of the 3_1^- state. Although the excitation energy of the 1^- state at a first glance seems inconsistent with such a picture, since it is higher than that of the 3_1^- state, this might be due to anharmonic effects.

The excitation energies and $B(E\lambda)$ values for the 5^- states as calculated by the QPM are listed in table 5. The structure of the reported 5^- states is very complicated. The first one-phonon state is equally distributed over the 5_1^-, the 5_2^-, the 5_3^- and the 5_5^- states. Moreover, each excitation contains about 50% two-phonon and 20% three-phonon contributions. The single exception is the 5_4^- state, which is almost purely built from the second one-phonon state. It is clear that the theoretical description of the 5^- states is very sensitive to the basis of one- and multi-phonon states which are included in the calculations and thus is a good test-case for the validity of the configuration space.

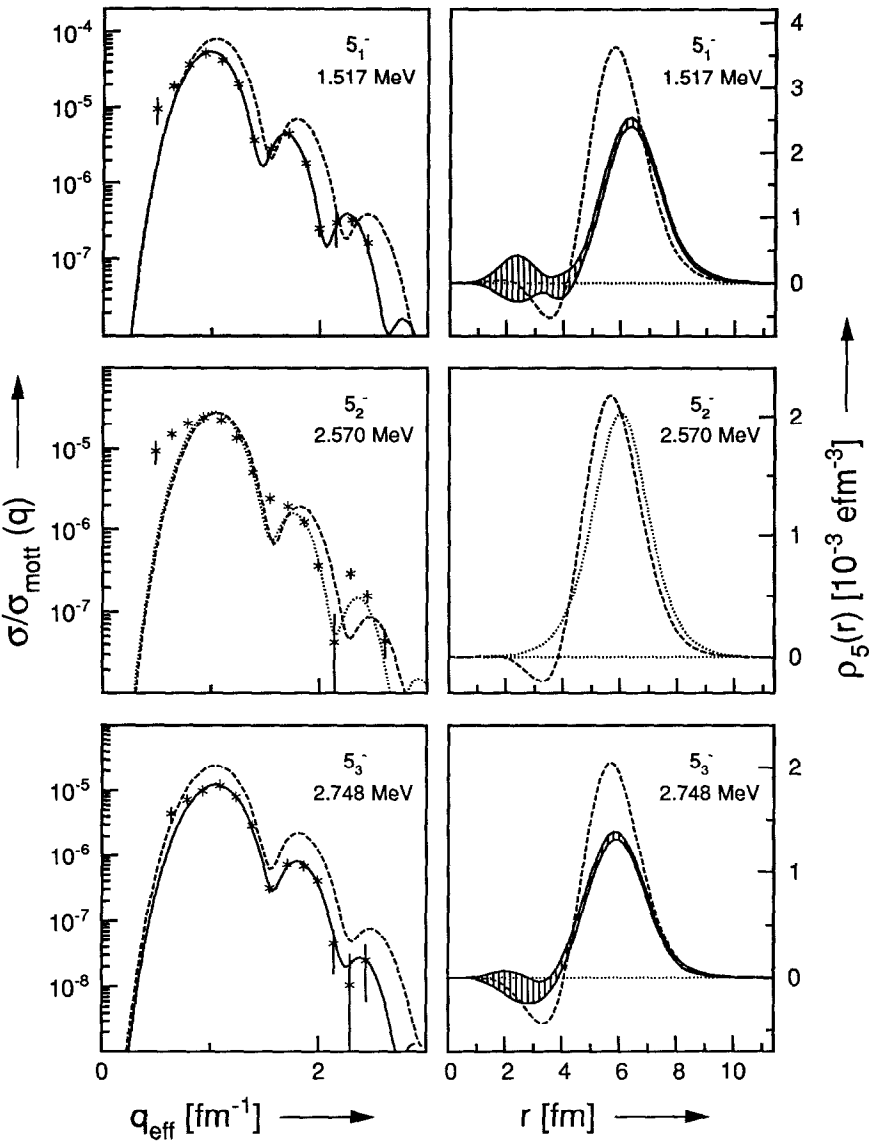

Fig. 12. Experimental form-factor data with the Fourier-Bessel fits (solid line) and the deduced transition charge densities (curves with error bands) of the 5^- states at 1.517, 2.570 and 2.748 MeV, compared to the results of the QPM calculations (dashed curves). The dotted curve for the 5_2^- state denotes the fit with a standard transition density. In the labeling of the states the transition at 2.046 MeV has been neglected.

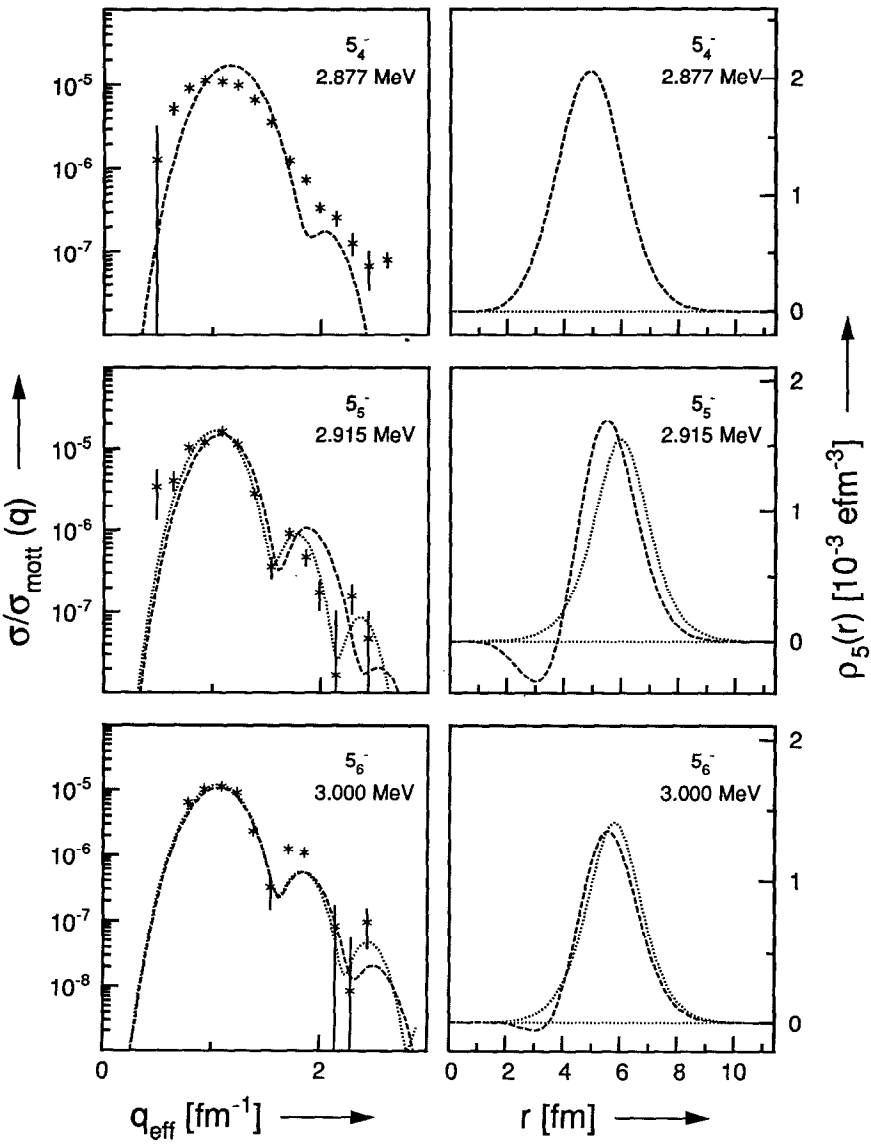

Fig. 13. Experimental form-factor data of the 5^- states at 2.877, 2.915 and 3.000 MeV, compared to the results of the QPM calculations represented by the dashed curves. The dotted curves denote the fits with a standard transition density. In the labeling of the transitions the state at 2.046 MeV has been neglected.

The agreement for the $B(E5)$ values is quite reasonable. The strength structure of one strong 5^- state and several higher 5^- states, more or less equally strong, is at least qualitatively observed. However, a 5^- state at 2.046 MeV is reported in the literature, which is not predicted by the QPM. This state is apparently only weakly excited, since it is not observed in the present experiment. The comparison of the transition charge densities and form factors, shown in figs. 12 and 13, is not so straightforward due to the large radius at which the transition charge density of the 5_1^- state peaks and the width of the first form-factor maximum of the 5_2^- state. If, however, the two states at 2.877 and 2.915 MeV, respectively, are assumed to be 5^- states (and the excitation at 2.046 MeV is not included) the structure of the densities as predicted by the QPM calculations is on the whole confirmed by the experimental data. Also the reasonable description of the form factor of the transition at 2.877 MeV shows that it is likely that at least one of the components of this peak, which possibly receives contributions from a number of levels, is a 5^- state. In figs. 12 and 13 the labeling of the 5^- states has been performed under the aforementioned assumptions.

In spite of the ambiguities in the identification of the experimental data with the calculated transitions, it can be concluded from the above that the configuration space used in the calculations is at least reasonable.

7. Comparison with RVM calculations

To investigate in how far ^{146}Nd can be regarded as a deformed nucleus with vibrations superposed, calculations were performed with the RVM. For the description of the ground-state charge density the Fermi parametrisation from ref. [16]) has been used. The deformation parameters, listed in table 6, have been determined in a similar fashion as described in ref. [11]). The resulting transition charge densities are compared to the experimental ones in fig. 14.

TABLE 6

The parameters, used in the RVM, to calculate the transition charge densities of the ground-state band, the γ-band and the octupole band in ^{146}Nd.

	Parameter	^{146}Nd
ground state	r_0 [fm]	1.074
charge density	a [fm]	0.632
ground-state band	β_2	0.142
	β_4	0.025
	β_6	–
γ-band	η_{22}	0.051
	η_{42}	0.067
octupole band	η_{30}	0.147
$(K=0)$	η_{50}	0.047
	ξ_{10}	−0.0172

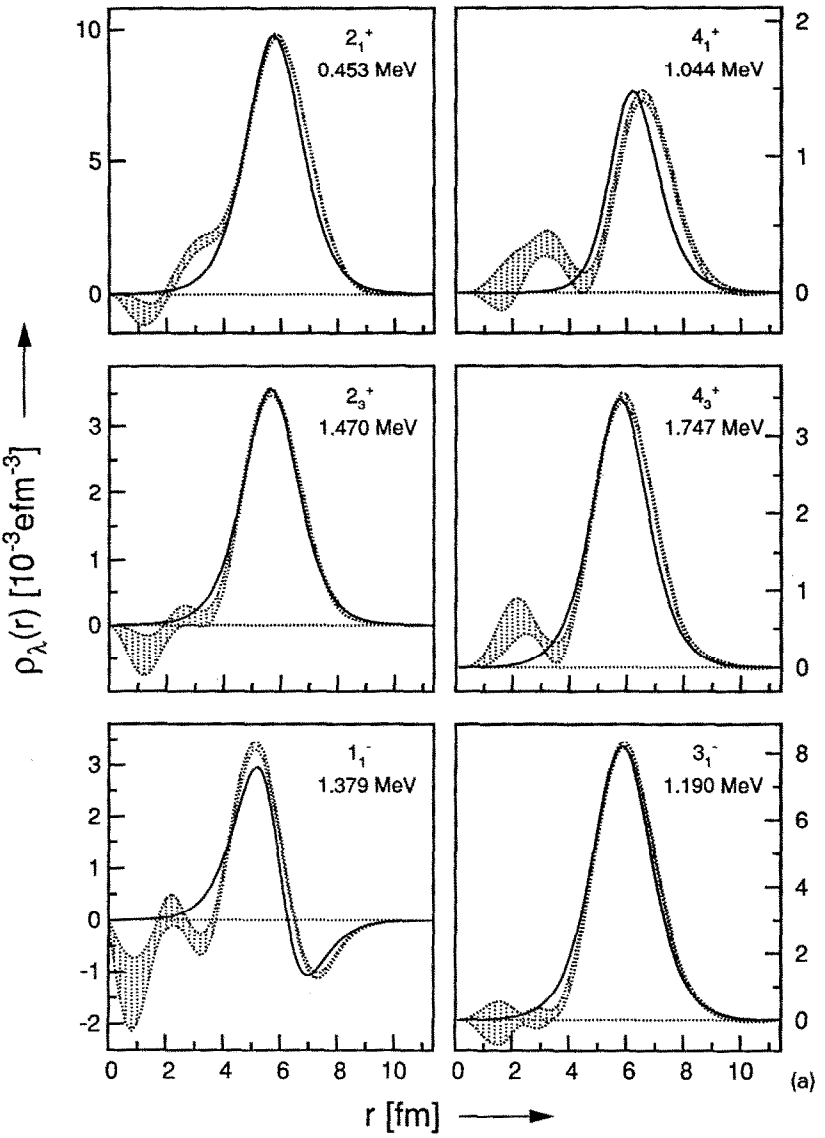

Fig. 14. Comparison between the experimental transition charge densities (curves with error bands) and the results of the calculations with the RVM (solid lines) for the 2^+ state at 0.453 MeV and the 4^+ state at 1.044 MeV of the ground-state band, the 2^+ state at 1.470 MeV and the 4^+ state at 1.747 MeV of the γ-band and the 1^- state at 1.379 MeV, the 3^- state at 1.190 MeV and the 5^- state at 1.517 MeV of the $K^\pi = 0^-$ octupole band.

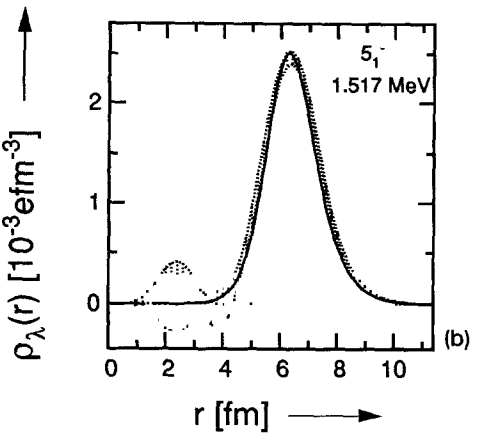

Fig. 14—continued

It can be observed that most features of the transition densities can be reproduced fairly well, with the exception of the radius at which the transition density of the $4^+_{g.s.}$ state peaks. It should be remarked, that the radial positions of the calculated transition charge densities of the 4^+_γ state and the 5^-_1 state are mainly determined by the values of η_{22} and η_{30}. The good agreement with the experimental transition densities suggests that the description of ^{146}Nd as a deformed nucleus and its excited states in terms of band structures is reasonable for the states of which the transition densities are shown in fig. 14.

The value of β_2 is consistent with the quadrupole deformation of ^{146}Nd determined by Coulomb excitation [21]. Moreover, it is in agreement with the value calculated by Caballero and Moya de Guerra [22] with the Strutinsky method [23]) and from a later calculation by the same group [24]) in the density-dependent Hartree-Fock approximation. The large η_{42} parameter needed to reproduce the strength of the 4^+_γ state is quite remarkable. This value is about a factor two larger than observed for any of the well-deformed nuclei in the rare-earth region [20]). It is, however, consistent with the extreme softness of the potential-energy surface (see fig. 1) in the γ-direction.

8. Summary and conclusions

The form factors of the low-lying states of ^{146}Nd with excitation energies up to 3.0 MeV have been measured for effective momentum transfers between 0.5 and 2.8 fm^{-1}. Some forty levels have been observed and for thirteen of them transition charge densities were obtained, whereas for sixteen more only form-factor data were presented. For most levels the form factors were consistent with the spin and parity assignments as given in the literature, although some ambiguities remain, such as

for instance the character of the state at 2.275 MeV. Table 7 lists all the states which have been observed in the present experiment.

The transition charge densities have been compared to two microscopic models, the quasiparticle-phonon model (QPM) and the density-dependent Hartree-Fock-Bogoliubov model (DDHFB) with a dynamical calculation of transition charge densities. The two models take a completely different approach in the sense that the QPM assumes a spherical nucleus and the DDHFB is most suitable for strongly deformed nuclei. Since ^{146}Nd has features of a vibrational as well as of a deformed nucleus, it is *a priori* to be expected that both models will have limited success in describing this nucleus.

The PES of the nuclear ground state as calculated by the DDHFB model shows a very soft minimum at $\beta = 0.15$ and $\gamma = 7°$ with another local minimum at $\beta = 0.1$ and $\gamma = 60°$. This, together with the low barrier between the two minima, indicates that the nucleus may change its shape drastically as a function of excitation energy.

A first indication is seen in the quadrupole states. The 2_1^+ state peaks at a larger radius than predicted by the QPM using the parameters of the Woods-Saxon potential of ^{142}Nd, even after correcting for the increase in size due to the four extra neutrons. The higher 2^+ states, though, all have experimental transition charge

TABLE 7

Summary of the excited states in ^{146}Nd, observed in the present experiment. The excitation energies and the $B(E\lambda)$ values are compared to the results of the QPM calculations.

Experiment		QPM			Experiment		QPM		
E_x [MeV]	$B(E\lambda)$ [$e^2fm^{2\lambda}$]	J^π	E_x [MeV]	$B(E\lambda)$ [$e^2fm^{2\lambda}$]	E_x [MeV]	B(Eλ) [$e^2fm^{2\lambda}$]	J^π	E_x [MeV]	$B(E\lambda)$ [$e^2fm^{2\lambda}$]
0.453	6.91×10^3	2_1^+	0.565	5.44×10^3	2.374				
1.044	1.50×10^6	4_1^+	0.870	1.42×10^6	2.437				
1.190	3.52×10^5	3_1^-	1.150	1.62×10^5	2.457				
1.303		2_2^+	1.640	2.42×10^1	2.484				
1.379	4.51×10^{-3}	1^-			2.530	2×10^4	3_3^-	3.010	4.92×10^2
1.470	6.8×10^2	2_3^+	2.150	1.06×10^3	2.570	8.5×10^7	5_2^-	2.520	5.25×10^7
1.517	2.64×10^8	5_1^-	1.670	1.91×10^8	2.622	3×10^5	4^+		
1.747	3.61×10^6	4_2^+	1.590	2.33×10^6	2.665	1.68×10^2	2^+		
1.789		2_4^+	2.360	1.84×10^1	2.690	5×10^3	3_4^-	3.180	6.26×10^3
1.919		4^+			2.709				
1.977	2×10^2	2_6^+	2.600	2.08×10^2	2.748	2.93×10^7	5_3^-	3.120	4.52×10^7
1.987	2.1×10^6	4_3^+	2.040	2.19×10^6	2.807		3_5^-	3.390	3.71×10^4
2.030					2.822		3_6^-	3.840	1.05×10^4
2.090					2.850	2×10^4	3^-		
2.152					2.877		5_4^-	3.170	1.39×10^7
2.198		2^+			2.915	4.7×10^7	5_5^-	3.510	1.97×10^7
2.231	3.84×10^1 [a]	0^+			2.935	1.6×10^6	4^+		
2.275		1^-			2.976	6×10^{-1}	2^+		
2.339	5.1×10^4	3_2^-	2.380	5.34×10^4	3.000	2.7×10^7	5_6^-	3.810	1.83×10^7

[a]) In units of e^2fm^4.

densities or form factors more or less in agreement with the calculations for a spherical nucleus. In this respect especially the good prediction of the strength distribution of the first six quadrupole states is a convincing argument that the dominating configurations contributing to quadrupole excitations are of a vibrational character with perhaps some single-particle degrees of freedom but, except for the 2_1^+ state, only little contribution of rotational degrees of freedom. Although the experimental situation for the octupole states is not resolved beyond doubt, it seems likely that the two 3^- states for which transition charge densities were presented, are indeed the first too octupole states as predicted by the QPM. However, the description of the 3^- states by the QPM is incomplete, probably due to too large cuts in the phonon basis, resulting in too few octupole states. As in the case of the quadrupole states the deformation seems to disappear or at least decrease for the second excited octupole state.

This is even more strongly observed in the hexadecapole states, where the first 4^+ state has a density which peaks well outside the average nuclear radius, suggesting a positive hexadecapole moment. The 4_2^+ state has a surface-peaked transition charge density with a B(E4) value more than twice that of the 4_1^+ state. This fact, in combination with the strength of the 4_4^+ state at 1.987 MeV, has been explained by the QPM as to arise from the lowering of the energy of the $[2_1^+ \times 2_1^+]^{(4)}$ and $[2_1^+ \times 4_1^+]^{(4)}$ two-phonon configurations below that of the first one-phonon state, due to their interaction with the three-phonon configurations. The QPM, however, misses the weakly excited hexadecapole state at 1.919 MeV.

In case of the 5^- states the QPM also misses the weak 5_2^- state. For the remaining states observed in the present experiment the overall agreement is reasonable. Both the fragmentation of 5^- strength and the radius at which the transition charge densities peak is generally well predicted. The most important discrepancy occurs for the transition charge density of the 5_1^- state, which has a maximum at a radius much larger than the average nuclear radius.

A general feature for multipolarities from 2 to 5 is that the transition charge density of the first state has a maximum at a much larger value than the average nuclear radius. From this a deformation can be deduced, which is supported by the measured quadrupole moment of the nucleus. Moreover, the transition charge densities of the higher excitations of the mentioned multipolarities all peak at a lower value than the first excited state. This points, just as in the case of ^{150}Nd, to excitation of rotational bands. To examine this further the experimental transtition charge densities were compared to the results of dynamical DDHFB calculations and calculations with the macroscopic rotation-vibration model (RVM).

It is observed, that the DDHFB calculations give quite a good description of the transition charge densities of the 2_1^+ and 4_1^+ states, while the agreement of the RVM with the experimental data is excellent. The only discrepancy of the latter calculations with the data is the position of the maximum of the transition charge density of the 4_1^+ state. Since the DDHFB predicts this position better, it is concluded that the

anomalously large radius is a consequence of the microscopic structure of the nucleus and points to an extreme softness with respect to quadrupole and hexadecapole excitations. The softness of ^{146}Nd with respect to vibrations with other multipolarities (3 and 5) is confirmed by the large values of the amplitude parameters obtained from the RVM, which are up to a factor 2 larger than for ^{150}Nd.

It is concluded that ^{146}Nd is a nucleus in which there is a shape coexistence of prolate-deformed and spherically symmetric shapes. The good description with the RVM and the DDHFB for the lowest state of each multipolarity shows that these are governed by rotational degrees of freedom. The structure of the transition charge densities of the higher excitations is reasonably well explained by the QPM, pointing to a vibrational character of this nucleus. Therefore, the nucleus is very soft and at higher energies the deformed nucleus turns spherical.

This work is part of the research program of the National Institute for Nuclear Physics and High-Energy Physics (NIKHEF-K) and the Foundation for Fundamental Research of Matter (FOM), which is financially supported by the Netherlands' Organization for Scientific Research (NWO).

References

1) H.S. Gertzman, D. Cline, H.E. Gove and P.M.S. Lesser, Nucl. Phys. **A151** (1971) 282
2) L. von Bernus, W. Greiner, V. Rezwani, W. Scheid, M. Seldmayr and R. Seldmayr, Proc. Top. Conf. on problems of vibrational nuclei, Zagreb, 1974, ed. G. Alaga, V. Paar and L. Sips (North-Holland, Amsterdam, 1975) p. 230
3) T.J. Al-Janabi, J.D. Jafar, H.M. Youhana, A.M. Demidov and L.I. Govor, J. of Phys. **G9** (1983) 779
4) D.M. Snelling and W.D. Hamilton, J. of Phys. **G9** (1983) 111
5) M. Pignanelli and R. De Leo, private communication, 1990
6) A. Ahmad, G. Bomar, H. Crowell, J.H. Hamilton, H. Kawakami, C.F. Maguire, W.G. Nettles, R.B. Piercey, A.V. Ramayya, R. Soundranayagam, R.M. Ronningen, O. Scholten and P.H. Stelton, Phys. Rev. **C37** (1988) 1836
7) H.H. Pitz, R.D. Heil, U. Kneissl, S. Lindenstruth, I. Seemann, R. Stock, C. Wesselborg, A. Zilges, P. von Brentano, S.D. Hoblit and A.M. Nathan, Nucl. Phys. **A509** (1990) 587
8) R.K.J. Sandor, H.P. Blok, U. Garg, M.N. Harakeh, C.W. de Jager, V.Yu. Ponomarev, A.I. Vdovin and H. de Vries, Phys. Lett. **B233** (1989) 54
9) R.K.J. Sandor, H.P. Blok, U. Garg, M.N. Harakeh, C.W. de Jager, V.Yu. Ponomarev, A.I. Vdovin and H. de Vries, Nucl. Phys. **A535** (1991) 669
10) R.K.J. Sandor, H.P. Blok, U. Garg, M. Girod, M.N. Harakeh, C.W. de Jager and H. de Vries, Phys. Rev. **C43** (1991) R2040
11) R.K.J. Sandor, H.P. Blok, M. Girod, M.N. Harakeh, C.W. de Jager and H. de Vries, Nucl. Phys., **A551** (1993) preceding article.
12) J.B.J.M. Lanen, Ph.D. Thesis, University of Utrecht, Utrecht, The Netherlands (1990), unpublished
13) A. Zaringhalam and J.W. Negele, Nucl. Phys. **A288** (1977) 417
14) L.K. Peker, Nucl. Data Sheets **60** (1990) 953
15) Y. Ikeda, H. Yamamoto, K. Kavada, T. Katoh and T. Nagahara, J. Phys. Soc. Jpn. **45** (1978) 725
16) J.H. Heisenberg, J.S. McCarthy, I. Sick and M.R. Yearian, Nucl. Phys. **A164** (1971) 340
17) R.H. Spear, At. Data Nucl. Data Tables **42** (1989) 55
18) J. Mieremet, Master's Thesis, University of Amsterdam, Amsterdam, The Netherlands (1990), unpublished
19) U. Götz, H.C. Pauli, K. Adler and K. Junker, Nucl. Phys. **A192** (1972) 1

20) T. Ichihara, H. Sakaguchi, M. Nakamura, M. Yosoi, M. Ieiri, Y. Takeuchi, H. Togawa, T. Tsutsumi and S. Kobayashi, Phys. Rev. **C36** (1987) 1754
21) P. Raghavan, At. Data Nucl. Data Tables **42** (1989) 189
22) J.A. Caballero and E. Moya de Guerra, Nucl. Phys. **A509** (1990) 117
23) V.M. Strutinsky, Nucl. Phys. **A218** (1974) 169
24) E. Moya de Guerra, P. Sarriguren, J.A. Caballero, M. Casas and D.W.L. Sprung, Nucl. Phys. **A529** (1991) 68